BNL-205757-2018-JAAM

Introducing Fe2+ into Nickel-Iron Layered Double Hydroxide: Local Structure Modulated Water Oxidation Activity

Z. Cai, S. Bak

To be published in "Angew Chem"

July 2018

Chemistry Department

Brookhaven National Laboratory

U.S. Department of Energy

USDOE Office of Energy Efficiency and Renewable Energy (EERE), Vehicle Technologies Office (EE-3V)

DISCLAIMER

Introducing Fe^{2+} into Nickel-Iron Layered Double Hydroxide: Local Structure Modulated Water Oxidation Activity

Zhao Cai,[†[a,b]] Daojin Zhou,[†[a]] Maoyu Wang,[†[c]] Seong-Min Bak,[[d]] Yueshen Wu,[[b]] Zishan Wu,[[b]] Yang Tian,[[a]] Xuya Xiong,[[a]] Yaping Li,[[a]] Wen Liu,[[a,b]] Samira Siahrostami,[[e]] Yun Kuang,[[a]] Xiao-Qing Yang,[[d]] Haohong Duan,*[[f]] Zhenxing Feng,*[[c]] Hailiang Wang,*[[b]] Xiaoming Sun*[[a,g]]

[a] Z. Cai,[[†]] D. Zhou,[[†]] Y. Tian, X. Xiong, Dr. Y. Li, Dr. W. Liu, Dr. Y. Kuang, Prof. X. Sun
State Key Laboratory of Chemical Resource Engineering, Beijing Advanced Innovation Center for Soft Matter Science and Engineering, Beijing University of Chemical Technology
Beijing 100029 (China)
E-mail: sunxm@mail.buct.edu.cn
[b] Z. Cai,[[†]] Y. Wu, Z. Wu, Dr. W. Liu, Prof. H. Wang
Department of Chemistry and Energy Sciences Institute, Yale University
West Haven, Connnecticut 06516 (United States)
E-mail: hailiang.wang@yale.edu
[c] M. Wang,[[†]] Prof. Z. Feng
School of Chemical, Biological, and Environmental Engineering, Oregon State University
Corvallis, Oregon 97331 (United States)
E-mail: zhenxing.feng@oregonstate.edu
[d] S. M. Bak, Prof. X. Q. Yang
Chemistry Division, Brookhaven National Laboratory
Upton, New York 11973 (United States)
[e] Prof. S. Siahrostami
SUNCAT Center for Interface Science and Catalysis, Department of Chemical Engineering, Stanford University
Stanford, California 94305 (United States)
[f] Dr. Haohong Duan
Chemistry Research Laboratory, Department of Chemistry, University of Oxford
Oxford, OX1 3TA (United Kingdom)
E-mail: haohong.duan@chem.ox.ac.uk
[g] Prof. X. Sun
College of Energy, Beijing University of Chemical Technology
Beijing 100029 (China)
[†] These authors contributed equally to this work.

Abstract: Exploring materials with regulated local structures and understanding how the atomic motifs govern the reactivity and durability of catalysts are a critical challenge for designing advanced catalysts. Here we report the tuning of the local atomic structure of nickel-iron layered double hydroxides (NiFe-LDHs) by partially

substituting Ni^{2+} with Fe^{2+} to introduce Fe-O-Fe moieties. These Fe^{2+}-containing NiFe-LDHs exhibit enhanced oxygen evolution reaction (OER) activity with an ultralow overpotential of 195 mV at the current density of 10 mA/cm^2, which is among the best OER catalytic performance reported to date. In-situ X-ray absorption, Raman, and electrochemical analysis jointly reveal that the Fe-O-Fe motifs could stabilize high-valent metal sites at low overpotentials, thereby enhancing the OER activity. These results reveal the importance of tuning the local atomic structure for designing high efficiency electrocatalysts.

Catalysts are typically multicomponent materials with complicated interactions[1]. To tune the local structure of active components has shown great potential to alter the performance besides components optimization[2]. For instance, in gas-phase catalytic reactions, different oxygen-bridged metal motifs (OBMM) exhibited various impacts[3]. Despite several recent studies on local structure modulation of single-atom Au/NiFe LDH and Fe-doped NiOOH, similar demonstration of OBMM in liquid-phase electrocatalysis is still rare[4]. Therefore, regulating local structures and the consequent atomic interactions inside an electrocatalyst to pursue unprecedented intrinsic activity is highly challenging, but intriguing and useful.

NiFe-LDH material, as a benchmark OER catalyst actively studied over the past decades[5], is a typical multicomponent system with Fe^{3+} centers surrounded and atomically isolated by Ni^{2+} sites, forming the OBMM of only Ni-O-Fe. In spite of the debates on the active sites (Ni vs. Fe) for OER[6], it is increasingly convinced that the combination/interactions of both Ni and Fe (Ni-O-Fe) play a vital role on optimizing the OER performance[7]. It would be informative and intriguing to introduce double sites of Fe to form Fe-O-Fe OBMM into Ni-based LDH matrix to see the local structure effects (Ni-O-Fe vs. Fe-O-Fe) with Ni/Fe ratio unchanged. However, the LDH expressed in the formula of $M^{2+}_{1-x}M^{3+}_{x}(OH)_2(A^{n-}_{x/n})\bullet mH_2O$ (A^{n-}: interlayer anion) typically has their M^{3+} ions atomically isolated by M^{2+} sites due to static repulsions[8], it is forbidden to form Fe^{3+}-O-Fe^{3+} motif inside LDH during synthesis. Hence, constructing Fe-O-Fe motifs within NiFe-LDH structure and understanding their role on electrocatalysis at atomic level is a challenging puzzle.

Herein, we employ mixture of Fe^{2+} and Fe^{3+} salts for coprecipitation with Ni^{2+} salt. By this, M^{2+}-positioned Ni could be replaced as Fe to form Fe-O-Fe motifs in NiFe-LDH and the local structure effect on OER activity could be investigated. Our electrochemical and Raman analysis demonstrate the Fe-O-Fe couple concentration in NiFe electrocatalyst ties closely with the OER performance, and growing them into array structure can further push the OER overpotential down to 195 mV (10 mA/cm^2), which is comparable to the best NiFe OER catalysts reported so far. In-situ spectroscopic characterization, together with density functional theory (DFT) studies further reveal that the Fe-O-Fe motifs would make high-valent metal sites stable at atomic-level, hence enhancing the OER performance. These results clearly demonstrate the important role of local atomic structure on optimizing NiFe-based OER electrocatalyst, which should be inspiring for other catalyst design or synthesis.

Computational study was firstly performed to foresee if the Fe-O-Fe OBMM has

beneficial effect on the OER catalysis theoretically. In LDH structure, trivalent metal sites are surrounded and atomically isolated by divalent metal atoms[8a, 8c]. As to NiFe LDH (Figure 1a), a central Fe^{3+} site is surrounded by six neighboring Ni atoms (Ni:Fe=2:1), thus only Ni-O-Fe couples present in traditional NiFe LDH. To introduce Ni-sited Fe atoms into NiFe LDH without altering the Ni/Fe ratio, we moved half of Fe atoms by one lattice to make them connected with neighboring Fe and let their own position occupied by Ni. Thus, by switching the positions of a Ni and Fe, Fe-O-Fe couple can be artificially constructed (Figure 1b). A typical OER process of NiFe catalyst in alkaline conditions goes through four elementary stages: M*, M-OH, M-O, and M-OOH (Figure 1c and S1). Figure 1d and Table S1 compare the calculated free energy of each OER elementary step occurring at corresponding metal sites in NiFe LDH structure. For the Ni site, the deprotonation of OH* to O* is a limiting step, resulting in calculated overpotential of 0.48 V. When Fe atom is considered as the active site, the formation of O* is facilitated with overpotential of 0.36 V, demonstrating Fe as the active site in NiFe LDH system, in agreement with previous reports[9]. When Ni-sited Fe atom is introduced, the overpotential is decreased (0.32 V), suggesting a further improvement on the OER activity. Therefore, by modulating the local atomic structure, we achieve a higher theoretical OER activity.

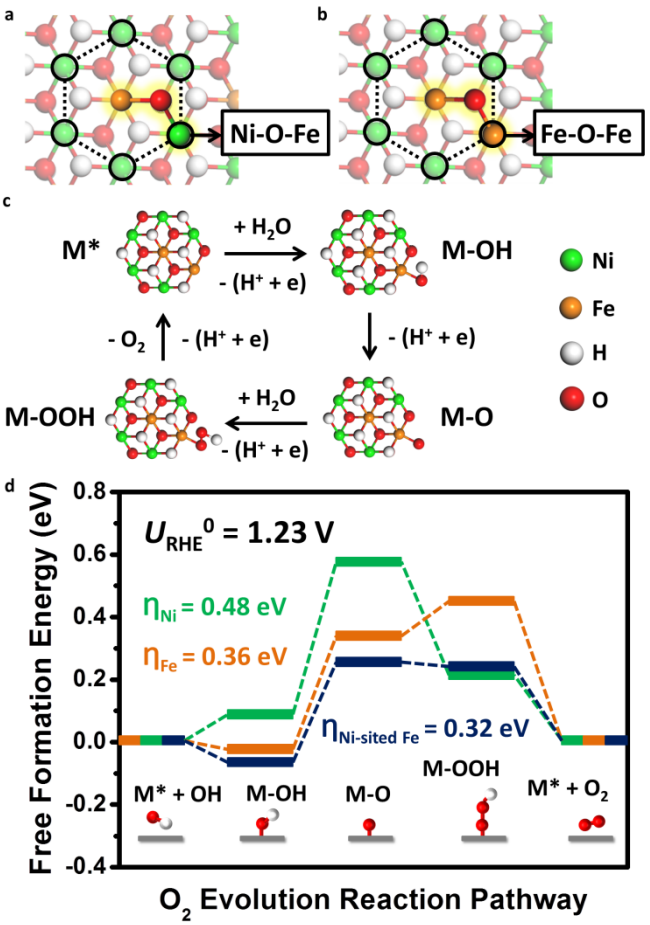

Figure 1. Atomic model of (a) traditional NiFe LDH and (b) NiFe LDH with Ni-sited Fe introduced. (c) Proposed OER pathway for NiFe LDH catalyst. (d) The calculated

OER free energy diagram on the three sites in NiFe LDH model. The lower free energy value suggests the higher OER intrinsic activity.

Inspired by the theoretical results, we sought to devise a controlled process to introduce Ni-sited Fe atoms into NiFe LDH structure but keep the Ni/Fe ratio (2:1) unchanged. Since $Fe(OH)_2$ are easy to be oxidized to Fe^{3+} when exposed to water and air (oxygen) conditions, we fully bubbled all the salt solutions with N_2 and sulfite was used as guest anion during co-precipitation procedure to bring Fe^{2+} into the host layer of NiFe LDH with strict feeding ratio. Transmission electron microscopy (TEM) demonstrates a nanosheet morphology of the Fe^{2+}-containing NiFe LDH (Fe^{2+}/Fe^{3+}=1:9 to 9:1, Figure 2a and Figure S2). High-resolution TEM (Figure S3) indicates that the typical sample with Fe^{2+}/Fe^{3+}=1:1 (here denoted as Fe^{2+}-NiFe LDH) shared thickness of ~2.4 nm, suggesting the ultrathin nature, similar to the traditional NiFe LDH (Figure S4). We note that the color of Fe^{2+}-NiFe LDH is changed upon Fe^{2+} addition even by naked eye. With the increasing Fe^{2+}-doping amount, the color of Fe^{2+}-NiFe LDH (Figure 2a inset) turned greener, indicating conversion from ferric hydroxide (reddish brown) to fougèrite or trébeurdenite (dark green)[10]. Meanwhile, with the increasing Fe^{2+} concentration, the optical band gap of Fe^{2+}-NiFe LDH catalyst turned smaller monotonously (Figure S5), indicating the better electro-conductivity. X-ray diffraction (XRD) exhibits the same Bragg reflections of Fe^{2+}-NiFe LDH and traditional NiFe LDH (Figure 2b), implying no structural deformation caused by Fe^{2+} substitution. The X-ray photoelectron spectroscopy (XPS) 2p scans of Ni for both NiFe LDH and Fe^{2+}-NiFe LDH exhibit the same oxidation states of +2 (Figure S6). Moreover, the binding energies of Fe^{2+} 2p3/2 and Fe^{3+} 2p3/2 peaks are respectively recorded at ~713.3 and 711.3 eV[11], where we can determine the Fe^{2+}/Fe^{3+} ratio as ~1:1, matched well with the feeding ratio of Fe^{2+}-NiFe LDH. In addition, the Fe^{2+}/Fe ratio based on XPS results is almost the same as the feeding ratio with different Fe2+ concentration (Figure 2d, S7-S8, and Table S2). Meanwhile, the zeta potentials[12] of Fe^{2+}-NiFe LDH colloid decrease with Fe^{2+}/Fe ratio increase (Figure 2d). All these results suggest that Fe^{2+} had been quantitatively introduced into NiFe LDH through our controlled synthesis.

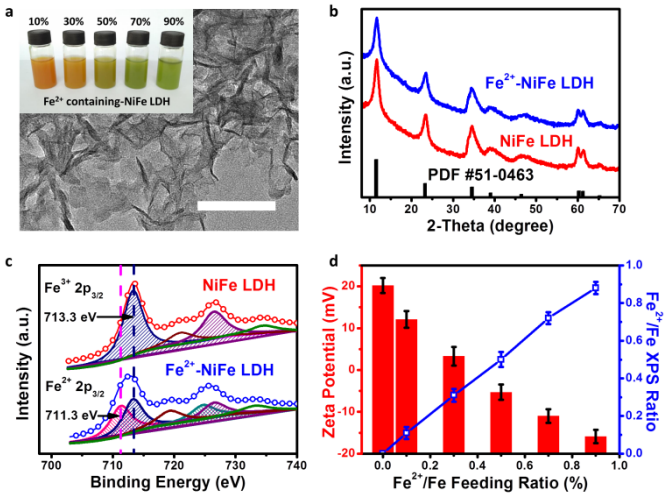

Figure 2. (a) TEM image of Fe^{2+}-NiFe LDH. Scale bar, 200 nm. The inset shows a digital image of as-prepared Fe^{2+}-NiFe LDH with different Fe^{2+} concentration. (b) XRD patterns of the traditional NiFe LDH and Fe^{2+}-NiFe LDH. (c) XPS analysis of Fe 2p in NiFe LDH and Fe^{2+}-NiFe LDH. (d) Zeta potential and Fe^{2+}/Fe XPS ratio of Fe^{2+}-NiFe LDHs with different Fe^{2+} concentrations, suggesting the quantitative introduction of Fe^{2+} sites.

IR-corrected OER polarization curves in Figure 3a exhibit a low overpotential of 249 mV at 10 mA/cm^2 for the Fe^{2+}-NiFe LDH, which is 79 mV lower than that of traditional NiFe LDH, suggesting an enhanced OER activity. The smaller Tafel slope (40.3 mV/dec, Figure 3a inset) and higher turnover frequency (TOF) at η = 300 mV (0.09 s^{-1}, Figure S9) further reveal the improved OER performance. In Nyquist plots (Figure S10), the Fe^{2+}-NiFe LDH shows a much smaller charge transfer resistance (3.8 Ω) than NiFe LDH (9.2 Ω), demonstrating an accelerated OER kinetics[13]. A stable current for Fe^{2+}-NiFe LDH catalyst is observed for 15 h operating, indicating a good long-term stability (Figure S11). The unchanged morphology and XRD pattern of Fe^{2+}-NiFe LDH after electrocatalysis further confirms the durability (Figure S12 and S13). The Ni/Fe ratio of Fe^{2+}-NiFe LDH after OER turned out to be 1.99:1, which is nearly the same as that before OER, evidencing no obvious leaching happens. Besides, the Fe^{2+}-NiFe LDHs with different Fe^{2+} concentrations showed nearly the same electrochemical active surface area (ECSA)[14] as NiFe LDH (Figure S14 and Table S3). Since their chemical composition, morphology, size, crystal structure (Figure S15) and ECSA had little difference, we attributed the enhanced OER activity of Fe^{2+}-NiFe LDH to the modulated local structure.

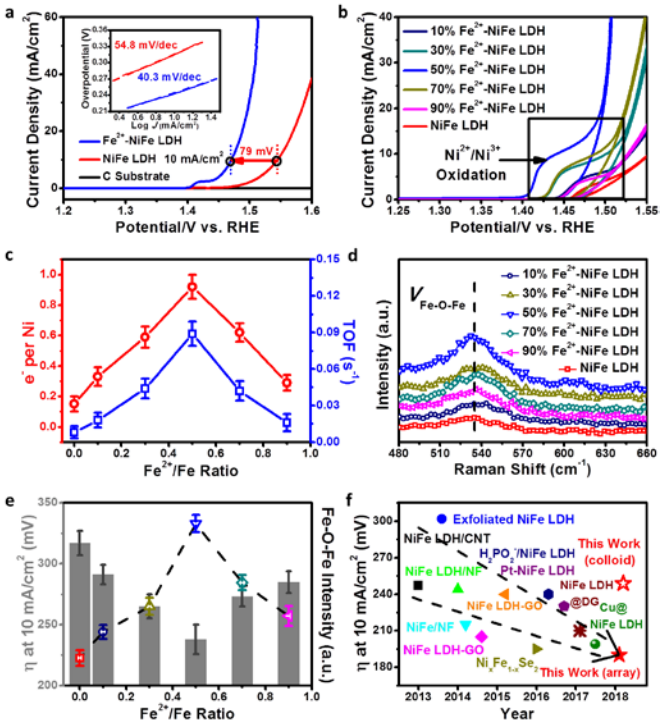

Figure 3. (a) Polarization curves of NiFe LDH and Fe^{2+}-NiFe LDH. The inset shows

the Tafel slopes of the two NiFe catalysts; (b) CV curves of Fe^{2+}-NiFe LDH with different Fe^{2+}/Fe ratio. (c) Electrons transferred per Ni atom and catalytic TOF at η = 300 mV of Fe^{2+}-NiFe LDH with different Fe^{2+}/Fe ratio. (d) Raman spectra and (e) OER overpotential at 10 mA/cm^2 vs. Fe-O-Fe concentration of Fe^{2+}-NiFe LDH with different Fe^{2+}/Fe ratios, demonstrating the Fe-O-Fe concentration-activity relationship. (f) Comparison of the OER overpotential at 10 mA/cm^2 of Fe^{2+}-NiFe LDH with reported NiFe-based OER catalysts.

The recyclable Ni^{2+}/Ni^{3+} oxidation peak at ~1.42 V[15] can be altered by their chemical environments and thus be a chemical index. The NiFe LDH with different Fe^{2+}/Fe ratio (xFe^{2+}-NiFe LDH, x=nFe^{2+}/nFe) were further analyzed to reveal the local structure-activity correlation. Comparing to traditional NiFe LDH, with the introduction of Fe^{2+} sites, 10%, 30%, and 50% Fe^{2+}-NiFe LDH exhibit improved OER activity gradually, meanwhile the Ni^{2+}/Ni^{3+} oxidation peak shifted to lower overpotentials (Figure 3b). But the higher Fe^{2+} concentration (Fe^{2+}/Fe^{3+} ratio > 1, i.e. 70% and 90% Fe^{2+}-NiFe LDH) means less central Fe^{3+} sites in LDH structure and is unfavorable to construct Fe-O-Fe linkages, leading to higher OER overpotential and positively-shifted Ni^{2+}/Ni^{3+} oxidation peak. After carefully studying the Ni^{2+}/Ni^{3+} oxidation electrons (i.e. e^- per Ni atom) and the OER intrinsic activity (i.e. TOF at η = 300 mV), we uncover the trend of the OER activity with respect to Ni oxidation state is quite similar (Figure 3c). This implies the introduction of Ni-sited Fe has regulated the local structure and made high-valent metal sites stable at low overpotentials. Raman characterization using Fe-O-Fe characteristic vibrations[16] at ~ 537 cm^{-1} (Figure 3d) as an index clearly indicates a strong positive correlation between the OER activity (i.e. overpotential at 10 mA/cm^2) and Fe-O-Fe concentration: the highest Fe-O-Fe concentration at 50% Fe^{2+}-NiFe LDH induces the strongest vibration, which is in coincidence with the lowest OER overpotential (Figure 3e). This makes clear that the introduction of Ni-sited Fe results in the construction of Fe-O-Fe linkage and the enhancement of the OER performance. Guided by the above results, we assemble the Fe^{2+}-NiFe LDH on Ni foam to further optimize the OER performance (Figure S16). The Fe^{2+}-NiFe LDH array electrode exhibits an impressively low OER overpotential of 195 mV at 10 mA/cm^2 (Figure 3f), which is so far among the best NiFe-based OER catalyst (Table S4), and much more active than the state-of-the-art IrO_2/C catalyst (Figure S17).

Operando X-ray Absorption spectrum (XAS)[17] was used to get further insight to the correlations between the local structure (Fe-O-Fe) and the enhanced OER activity. In Figure 4a, the X-ray absorption near edge structure (XANES) spectra of the Ni K-edge shows a valance state of +2 for Ni before catalysis. It shifts to +3 when a potential of 1.5 V is applied. When lowering the potential back to 0 V, Ni valence state turned back to +2 again. While for the Fe K-edge (Figure 4b), the Fe species in Fe^{2+}-NiFe LDH before applying potential (0 V) exhibits a mixed valance state of both +2 and +3. This matches well with our XPS results (Figure 2c). Noticeably, the iron's valance in Fe^{2+}-NiFe LDH turned +3 at 1.5 V, and kept the +3 state even when the potential went back to 0 V. By zooming in Figure 4b, the XANES edges of the

catalyst at 1.5 V are slightly at the right of that of Fe_2O_3 reference, indicating a valence state of Fe a bit higher than +3 (i.e. $Fe^{(3+\delta)+}$, where $\delta>0$). Moreover, the δ is calculated to be 0.22 though the integral method[18], demonstrating 22% of the total Fe species turned out to be Fe^{4+} during OER (Figure S18). This is in accord with previous finding using Mössbauer spectroscopy that partial Fe^{4+} existed during steady-state water oxidation[6c].

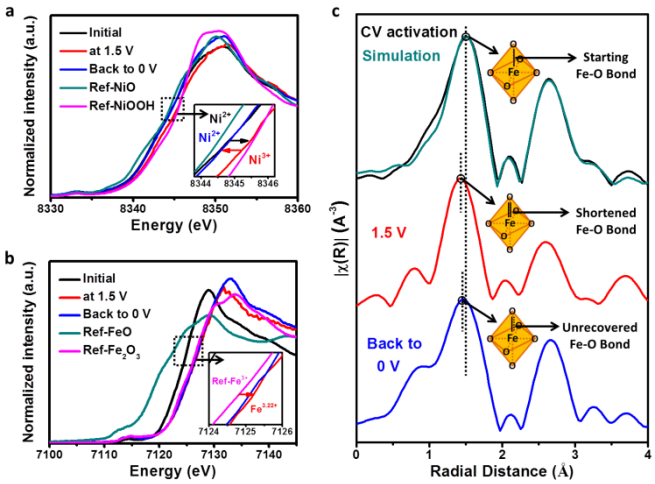

Figure 4. In situ-XANES spectra of (a) the Ni K-edge and (b) the Fe K-edge for the Fe^{2+}-NiFe LDH catalyst. The inset of (a) and (b): the enlarged absorption edge, demonstrating the Ni/Fe valance change. (c) the k^{2}-weighted Fourier-transformed data of Fe^{2+}-NiFe LDH catalyst under OER working condition, demonstrating the Fe-O bond length variation.

Recent studies have proposed that high-valent metal species (e.g. Fe^{4+} with unusual shorter Fe-O bonds) are the possible OER active site in NiFe system[2b, 6a, 6c]. In contrast to the $Fe^{3.22+}$ for Fe^{2+}-NiFe LDH at 1.5 V vs. RHE, the Fe species in traditional NiFe LDH show little valence change during OER (Figure S19). This revealed the redox behavior difference between Fe-O-Fe motifs with isolated Fe[6a, 6b]. To further confirm the local coordination environment, especially the Fe local structure, we analyzed the extended X-ray absorption fine structure (EXAFS) of Fe^{2+}-NiFe LDH (Figure 4c). The R-space EXAFS curve of Fe^{2+}-NiFe LDH after CV activation overlays with the simulated R-space curve using the atomic structure shown in Figure 1b. Similar agreement is also found in the K-space (Figure S20 and Table S5). This indicates that activated Fe^{2+}-NiFe LDH catalyst is the as-designed LDH atomic structure with typical M-O coordination. Under OER working condition, the Fe-O bond turned obviously shorter, which should be attributed to the high-valence $Fe^{(3+\delta)+}$ species and might contribute to the high OER performance. When the potential went back to 0 V, the Fe-O bond is still shorter than the starting case, in consist with the XANES results that the valence state of Fe is still higher than +3 in a short time after OER.

In summary, we demonstrate modulating local structure within LDH structure as an

effective strategy to improve the OER activity of NiFe catalyst. By means of electrochemical analysis, in-situ XAS, and DFT studies, we show the introduction of Ni-sited Fe atoms into NiFe LDH results in the formation of Fe-O-Fe couples, which act as stable high-valent motifs and are responsible for the significantly improved OER intrinsic activity. Our work reveals the important role of local structure on tuning the surface coordination environment for electrocatalysis optimization. The approach should be general and have implications for designing advanced electrocatalysts with favorable atomic arrangement.

Acknowledgements
This study was supported by the Natural Science Foundation of China, the Program for Changjiang Scholars and Innovative Research Team in the University, and the long-term subsidy mechanism from the Ministry of Finance and the Ministry of Education of P. R. China. The work at BNL was supported by the U.S. Department of Energy, the Assistant Secretary for Energy Efficiency and Renewable Energy, Office of Vehicle Technologies under Contract Number DE-SC0012704. Z. F. thanks the Callahan Faculty Scholar Endowment Fund from Oregon State University. XAS measurements were performed at 9-BM of Advanced Photon Source (APS), Argonne National Laboratroy (ANL). The use of APS of ANL is supported by DOE under Contract No. DE-AC02-06CH11357.

Keywords: NiFe catalyst • Local structure • Layered double hydroxide • Oxygen evolution

[1] a) C. C. McCrory, S. Jung, J. C. Peters, T. F. Jaramillo, J. Am. Chem. Soc. 2013, 135, 16977-16987; b) F. Song, X. Hu, J. Am. Chem. Soc. 2014, 136, 16481-16484; c) M. Gong, H. Dai, Nano Res. 2015, 8, 23-39.
[2] a) Y. H. Li, P. F. Liu, L. F. Pan, H. F. Wang, Z. Z. Yang, L. R. Zheng, P. Hu, H. J. Zhao, L. Gu, H. G. Yang, Nat. Commun. 2015, 6, 8064; b) M. B. Stevens, C. D. Trang, L. J. Enman, J. Deng, S. W. Boettcher, J. Am. Chem. Soc. 2017, 139, 11361-11364.
[3] a) M. W. Grinstaff, M. G. Hill, J. A. Labinger, H. B. Gray, Science 1994, 264, 1311-1313; b) E.-M. El-Malki, R. Van Santen, W. Sachtler, J. Catal. 2000, 196, 212-223; c) S. Yin, Z. Wang, E. R. Bernstein, J. Chem. Phys. 2013, 139, 084307.
[4] a) J. Zhang, J. Liu, L. Xi, Y. Yu, N. Chen, S. Sun, W. Wang, K. M. Lange, B. Zhang. J. Am. Chem. Soc. 2018, 140, 3876-3879; b) H. Shin, H. Xiao, W. A. Goddard. J. Am. Chem. Soc. 2018, 140, DOI: 10.1021/jacs.8b02225.
[5] a) D. Zhou, Z. Cai, X. Lei, W. Tian, Y. Bi, Y. Jia, N. Han, T. Gao, Q. Zhang, Y. Kuang, Adv. Energy Mater. 2017, 7, 1701905; b) M. Luo, Z. Cai, C. Wang, Y. Bi, L. Qian, Y. Hao, L. Li, Y. Kuang, Y. Li, X. Lei, Nano Res. 2017, 10, 1732-1739; c) Yu, L.; Yang, J. F.; Guan B. Y.; Lu, Y.; Lou, X. Angew. Chem. Int. Edit. 2018, 57, 178-182; d) F. Song, X. Hu, Nat. Commun. 2014, 5, 4477.
[6] a) D. Friebel, M. W. Louie, M. Bajdich, K. E. Sanwald, Y. Cai, A. M. Wise, M.-J. Cheng, D. Sokaras, T.-C. Weng, R. Alonso-Mori, J. Am. Chem. Soc. 2015, 137, 1305-1313; b) M. Görlin, P. Chernev, J. Ferreira de Araújo, T. Reier, S. r. Dresp, B.

Paul, R. Krähnert, H. Dau, P. Strasser, J. Am. Chem. Soc. 2016, 138, 5603-5614; c) J. Y. Chen, L. Dang, H. Liang, W. Bi, J. B. Gerken, S. Jin, E. E. Alp, S. S. Stahl, J. Am. Chem. Soc. 2015, 137, 15090-15093; d) V. Fidelsky, M. C. Toroker, Phys. Chem. Chem. Phys. 2017, 19, 7491-7497; e) Y. Elbaz, M. C. Toroker, J. Phys. Chem. C 2017, 121, 16819-16824.
[7] F. Dionigi, P. Strasser, Adv. Energy Mater. 2016, 6, 1600621.
[8] a) P. J. Sideris, U. G. Nielsen, Z. Gan, C. P. Grey, Science 2008, 321, 113-117; b) Q. Wang, D. O'Hare, Chem. Rev. 2012, 112, 4124-4155; c) G. Fan, F. Li, D. G. Evans, X. Duan, Chem. Soc. Rev. 2014, 43, 7040-7066.
[9] Y. Bi, Z. Cai, D. Zhou, Y. Tian, Y. Kuang, Y. Li, X. Sun, X. Duan, J. Catal. 2018, 358, 100-107.
[10] J.-M. R. Génin, O. Guérin, A. Herbillon, E. Kuzmann, S. Mills, G. Morin, G. Ona-Nguema, C. Ruby, C. Upadhyay, Hyperfine Interac. 2012, 204, 71-81.
[11] T. Yamashita, P. Hayes, Appl. Surf. Sci. 2008, 254, 2441-2449.
[12] Y. Zhou, X. Sun, K. Zhong, D. G. Evans, Y. Lin, X. Duan, Ind. Eng. Chem. Res. 2012, 51, 4215-4221.
[13] Z. Cai, Y. Bi, E. Hu, W. Liu, N. Dwarica, Y. Tian, X. Li, Y. Kuang, Y. Li, X. Q. Yang, Adv. Energy Mater. 2018, 8. 1701694.
[14] C. G. Morales-Guio, L. Liardet, X. Hu, J. Am. Chem. Soc. 2016, 138, 8946-8957.
[15] M. Görlin, J. Ferreira de Araújo, H. Schmies, D. Bernsmeier, S. r. Dresp, M. Gliech, Z. Jusys, P. Chernev, R. Kraehnert, H. Dau, J. Am. Chem. Soc. 2017, 139, 2070-2082.
[16] a) C. Tang, H. S. Wang, H. F. Wang, Q. Zhang, G. L. Tian, J. Q. Nie, F. Wei, Adv. Mater. 2015, 27, 4516-4522; b) J. Zhao, J. Chen, S. Xu, M. Shao, Q. Zhang, F. Wei, J. Ma, M. Wei, D. G. Evans, X. Duan, Adv. Funct. Mater. 2014, 24, 2938-2946.
[17] a) Z. Weng, Y. Wu, M. Wang, J. Jiang, K. Yang, S. Huo, X.-F. Wang, Q. Ma, G. W. Brudvig, V. S. Batista, Nat. Commun. 2018, 9, 415; b) C. Wei; Z. Feng; M. Baisariyev; L. Yu; L. Zeng; T. Wu; H. Zhao; Y. Huang; M. J. Bedzyk; T. Sritharan; Z. J. Xu. Chem. Mater. 2016, 28, 4129.
[18] H. Dau, P. Liebisch, M. Haumann, Anal. Bioanal. Chem. 2003, 376, 562-583.